ARTICLE

Tumor-expressed B7-H3 mediates the inhibition of antitumor T-cell functions in ovarian cancer insensitive to PD-1 blockade therapy

Dongli Cai[1,2], Jiaming Li[3], Dingfeng Liu[4], Shanjuan Hong[2], Qin Qiao[2], Qinli Sun[2], Pingping Li[4], Nanan Lyu[5], Tiantian Sun[3], Shan Xie[2], Li Guo[3], Ling Ni[2], Liping Jin[1,4] and Chen Dong[2,6]

Although PD-L1/PD-1 blockade therapy has been approved to treat many types of cancers, the majority of patients with solid tumors do not respond well, but the underlying reason remains unclear. Here, we studied ovarian cancer (OvCa), a tumor type generally resistant to current immunotherapies, to investigate PD-1-independent immunosuppression. We found that PD-L1 was not highly expressed in the tumor microenvironment (TME) of human OvCa. Instead, B7-H3, another checkpoint molecule, was highly expressed by both tumor cells and tumor-infiltrating antigen-presenting cells (APCs), which correlated with T-cell exhaustion in patients. Using ID8 OvCa mouse models, we found that B7-H3 expressed on tumor cells, but not host cells, had a dominant role in suppressing antitumor immunity. Therapeutically, B7-H3 blockade, but not PD-1 blockade, prolonged the survival of ID8 tumor-bearing mice. Collectively, our results demonstrate that tumor-expressed B7-H3 inhibits the function of $CD8^+$ T cells and suggest that B7-H3 may be a target in patients who are not responsive to PD-L1/PD-1 inhibition, particularly OvCa patients.

Keywords: Antitumor immunity; Immune checkpoint; B7-H3; T-cell exhaustion; Ovarian cancer

Cellular & Molecular Immunology (2020) 17:227–236; https://doi.org/10.1038/s41423-019-0305-2

INTRODUCTION

Tumors evade immune control via inhibitory checkpoint molecules that promote T-cell exhaustion.[1] Blockade of these inhibitory molecules to different degrees can reinvigorate T-cell functions and unleash antitumor immunity.[2] Specifically, blocking the interaction of PD-1 with its ligand PD-L1 shows potent and durable antineoplastic effects on a wide spectrum of tumors.[3] However, not all patients or tumor types respond to PD-1 inhibitor treatment equally, as shown by variable objective response rates (ORRs).[4] High PD-L1 expression in the tumor microenvironment (TME) has been reported to correlate favorably with the clinical benefits of PD-L1/PD-1 blockade therapies.[5] For example, the ORRs were 67–100% in PD-L1-positive non-small-cell lung cancer (NSCLC) patients vs. 0–15% in PD-L1-negative NSCLC patients,[6] 44–51% in PD-L1-positive melanoma patients vs. 6–17% in PD-L1-negative melanoma patients[6], and 18–31% in PD-L1-positive renal cell carcinoma (RCC) patients vs. 9–18% in PD-L1-negative RCC patients.[7,8] These data suggest that PD-1-independent immunosuppressive mechanisms that inhibit antitumor immunity in cancer patients may exist.

Ovarian cancer (OvCa) is an aggressive malignancy refractory to standard treatments and current immunotherapies.[9] In recent years, there have been no major advancements in the treatment of OvCa, and cytoreductive surgery followed by taxane/platinum-based chemotherapy or neoadjuvant chemotherapy and interval debulking surgery is still the standard of care.[10] OvCa has been shown to be immunogenic[11] and capable of eliciting a spontaneous antitumor immune response.[12,13] The quality of tumor-infiltrating T cells was shown to be a critical determinant of clinical outcomes in OvCa patients.[11,14,15] However, the efficacy of PD-L1/PD-1 blockade in OvCa has been more modest than that in the aforementioned tumor types,[16] with ORRs of only 11.5–12.3% in PD-L1-positive OvCa patients vs. 5.9% in PD-L1-negative OvCa patients.[17] In the JAVELIN study, the best ORR among 124 assessable patients with refractory/recurrent OvCa treated with avelumab (an anti-PD-L1 antibody) was 9.7%.[18] Similarly, in the KEYNOTE-028 trial, among 26 patients with PD-L1-positive OvCa treated with pembrolizumab (an anti-PD-1 antibody), the ORR was 11.5%.[19] According to these data, the response rates of anti-PD-1 and anti-PD-L1 antibodies in OvCa are not better than those of conventional therapies. Interestingly, in mice bearing ID8 tumors, the most commonly used OvCa mouse model of epithelial papillary serous adenocarcinoma, the PD-L1/PD-1 pathway blockade alone achieved little therapeutic effect compared with control treatment.[20–23] The need to elucidate the mechanisms underlying the unsatisfactory efficacy of the PD-L1/PD-1 pathway blockade and identify novel immunotherapeutic targets in OvCa is quite urgent.

[1]Obstetrics & Gynecology Hospital, Fudan University, Shanghai 200011, China; [2]Institute for Immunology and School of Medicine, Tsinghua University, Beijing 100084, China; [3]Suzhou Kanova Biopharmaceutical Co., Ltd, Suzhou 215000, China; [4]Clinical and Translational Research Center, Shanghai First Maternity and Infant Hospital, Tongji University School of Medicine, Shanghai 201204, China; [5]Department of Gynecologic Oncology, Beijing Obstetrics and Gynecology Hospital, Capital Medical University, Beijing, China and [6]Beijing Key Lab for Immunological Research on Chronic Diseases, Beijing 100084, China
Correspondence: Ling Ni (lingni@tsinghua.edu.cn) or Liping Jin (jinlp01@163.com) or Chen Dong (chendong@tsinghua.edu.cn)

Received: 28 April 2019 Accepted: 17 September 2019
Published online: 14 October 2019

B7-H3 (CD276 or B7RP-2) is a member of the B7 family that has 20–27% amino acid identity with other B7 family members.[24,25] The unidentified receptor(s) for B7-H3 has been reported to be expressed on activated T cells.[24,25] Aberrant B7-H3 expression has been reported in the vast majority of human malignancies, including melanoma,[26] RCC[27], and OvCa.[28] B7-H3 is constitutively expressed on immune cells, specifically antigen-presenting cells (APCs),[29] and can be induced on dendritic cells (DCs) after culture with regulatory T cells,[30] LPS, or IFN-γ.[31] APC-expressed B7-H3 has been reported to promote tumor progression by inhibiting the functions of $CD8^+$ T cells and NK cells.[29] Blockade of B7-H3 on APCs has potent therapeutic effects and can synergize with anti-PD-1 therapy in multiple mouse tumor models.[29] In addition, in the TME, B7-H3 expression has also been detected on tumor-associated vascular cells and tumor cells.[32] In OvCa, high expression of B7-H3 has mostly been verified only at the tissue level. B7-H3-positive tumor vasculature in OvCa is associated with the high-grade serous histological subtype, increased recurrence, and reduced survival.[28] The reported data suggest that in OvCa, B7-H3 is mostly expressed by tumor cells and promotes the invasion, migration, and proliferation of tumor cells.[33] However, there is no study on B7-H3 expression by OvCa-infiltrating immune cells. Furthermore, whether B7-H3 mediates immune evasion in cancer models or patients resistant to PD-1 blockade therapies has yet to be studied.

Here, we assessed the expression of B7 checkpoint molecules in OvCa and found that B7-H3, but not PD-L1, was highly expressed, which was associated with dysfunction in tumor-infiltrating T cells. In the ID8 model, tumor-intrinsic B7-H3 directly suppressed $CD8^+$ T-cell functions, and an anti-B7-H3 neutralizing antibody but not an anti-PD-1 antibody prolonged the survival of ID8 tumor-bearing mice. Our results thus uncover a critical role for B7-H3 on OvCa cells in suppressing antitumor immunity and offer a new immunotherapeutic target for patients resistant to PD-L1/PD-1 blockade therapy.

RESULTS

B7-H3 but not PD-L1 is robustly expressed in human OvCa

OvCa patients have a relatively unsatisfactory clinical response to immunotherapies, including PD-L1/PD-1 blockade.[13] Considering that several other B7 family checkpoint molecules have been implicated in antitumor immunity, we hypothesized that they may play important roles and account for the poor efficacy of PD-L1/PD-1 blockade therapy in OvCa. We first evaluated the mRNA expression of all ten reported B7 family members in human OvCa by GEPIA using data from the TCGA. We found that tumor tissues (tumor cells, tumor-associated APCs, tumor-infiltrating lymphocytes, etc.) from human OvCa patients had low mRNA expression of *CD274* (encoding PD-L1), but substantial mRNA expression of *CD276* (encoding B7-H3), *VTCN1* (encoding B7S1), and *C10orf54* (encoding VISTA) compared with other B7 family members (Fig. 1a). It is noteworthy that in human OvCa, *CD276* had the highest expression among all the tested B7 family members (Fig. 1a). Moreover, the mRNA levels of *CD274*, *CD276*, and *C10ofr54* in the tumor tissues were similar to those in normal control tissues, while the mRNA level of *VTCN1* in the tumor tissues was significantly higher than that in the normal tissues (Fig. 1b). We then examined the protein expression levels of these members in human OvCa by immunofluorescence. Tumor specimens were collected from 32 treatment-naive patients who fulfilled the study criteria. The clinical and pathological characteristics of the patients are summarized in Supplementary Table S1. Compared with normal ovarian tissues, the tumor specimens showed upregulated expression of PD-L1, B7-H3, B7S1, and VISTA (Fig. 1c, d). Consistent with the mRNA expression data, the protein expression level of PD-L1 in human OvCa was moderate, while that of B7-H3 was the highest among the levels of the evaluated molecules (Fig. 1c, d). These data indicate that B7-H3 but not PD-L1 is robustly expressed in human OvCa.

The efficacy of PD-L1/PD-1 blockade therapies has been reported to positively correlate with the expression of PD-L1.[3,34] In human OvCa specimens, the majority of PD-L1-expressing cells did not express pancytokeratin, which was used as an epithelial and therefore ovarian cell marker (indicated by the yellow arrows) (Fig. 1c). Analysis of the expression of PD-L1 on human OvCa cell lines (A2780 and SKOV3 cells) and freshly isolated primary OvCa cells also confirmed that OvCa tumor cells exhibited very low, if any, expression of PD-L1 (SI Appendix, Supplementary Fig. S1A). In $CD45^+$ cells isolated from OvCa tumors, PD-L1 was mainly expressed on lineage$^-$HLA-DR^{hi} dendritic cells (DCs) and $CD14^+$HLA-DR^{hi} macrophages/monocytes (Mø/Mo). However, the percentages of PD-$L1^+$ DCs and PD-$L1^+$ Mø/Mo in the tumors were not high, and there were no obvious differences in the ascites or PBMCs among the OvCa patients (SI Appendix, Supplementary Fig. S1B, C). As IFN-γ has been reported to upregulate PD-L1 expression on human OvCa cells,[35] it cannot be excluded that the low/nonexistent level of PD-L1 expression on primary cells isolated from OvCa was the result of a lack of exposure to an IFN-γ-rich TME. Generally, the low mRNA and protein levels of PD-L1 in OvCa may underscore the poor responsiveness to PD-L1/PD-1 blockade.

As shown in Fig. 1c, B7-H3 was highly expressed on both CD45-negative and CD45-positive cells (indicated by the white arrows); $CD45^+$B7-$H3^+$ and $CD45^-$B7-$H3^+$ cell infiltration into the OvCa TME showed no obvious difference (SI Appendix, Supplementary Fig. S1D). Consistent with the reported data, B7-H3 was found to be substantially expressed on seven human OvCa cell lines and freshly isolated primary OvCa cells (SI Appendix, Supplementary Fig. S1E), and B7-H3 exhibited higher expression than B7S1, VISTA, or PD-L1 (SI Appendix, Supplementary Fig. S1A). To better understand the expression pattern of B7-H3 on lymphocytes, we then used flow cytometry to assess the expression of B7-H3 on $CD45^+$ cells isolated from the tumors, ascites, and PBMCs of OvCa patients. B7-H3 was predominantly expressed on myeloid dendritic cells (mDCs), $CD14^+$HLA-DR^{hi} Mø/Mo, and $CD14^+$HLA-$DR^{low/-}$ monocytic myeloid-derived suppressor cells (mMDSCs). The percentages of B7-H3-expressing APCs in the tumors were generally higher than those in the ascites and peripheral blood (Fig. 1e). Moreover, the population of tumor-associated APCs in the ascites that expressed B7-H3 was mainly observed to comprise $CD14^+$HLA-DR^{hi} Mø/Mo (Fig. 1e). Consistent with the immunofluorescence results, in the tumors of the OvCa patients, APCs expressed higher levels of B7-H3 than B7-S1, VISTA, or PD-L1 (data not shown). These data confirm the robust expression of B7-H3 in human OvCa and suggest that in human OvCa, B7-H3 may play a more important role than PD-L1 in controlling antitumor immunity.

B7-H3 expression in human OvCa correlates with $CD8^+$ T-cell exhaustion

B7-H3 was previously reported to bind to a putative receptor on activated T cells[24,25] and inhibit their proliferation and function.[36,37] To understand the potential target cells of B7-H3 in OvCa, we utilized a biotinylated human B7-H3-mIgG2a Fc fusion protein to assess the expression of a putative B7-H3 receptor (B7-H3R). B7-H3R expression was detected on $CD4^+$ T, $CD8^+$ T, NK, and NKT cells in human OvCa (Fig. 2a), and B7-H3R expression was upregulated on tumor-infiltrating $CD4^+$ and CD8 T^+ cells compared with those in the ascites and peripheral blood (Fig. 2b). The distributions of B7-H3 and B7-H3R strongly suggest an important role for B7-H3 in regulating T cells in the OvCa microenvironment.

Inhibitory receptors on T cells have been associated with T-cell exhaustion in a chronic virus infection model and cancer patients.[1] To understand the regulatory role of B7-H3 in T cells, we

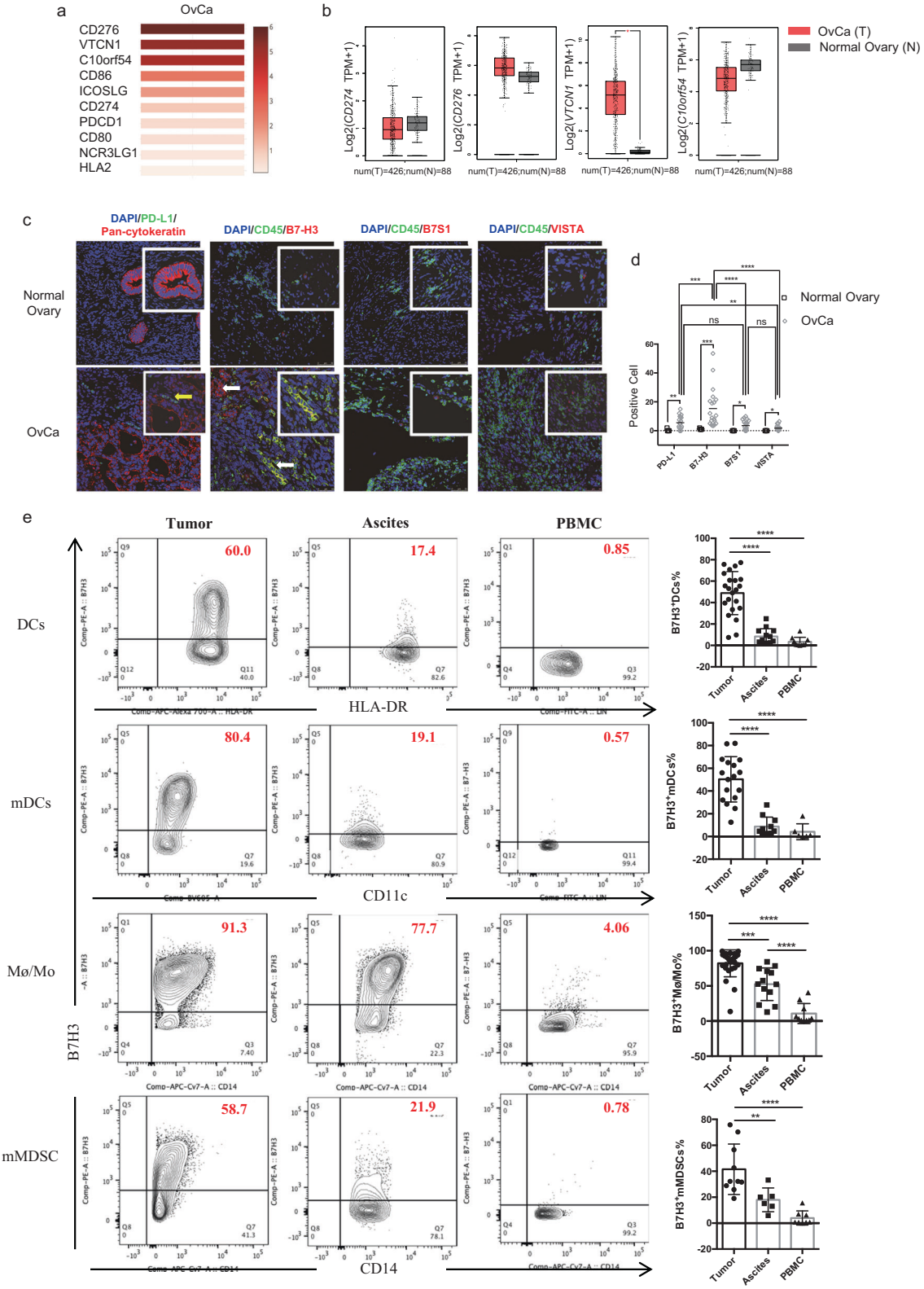

Fig. 1 B7-H3, but not PD-L1, is robustly expressed in human OvCa. **a** Heatmap analysis of the mRNA expression of B7 family genes in OvCa tumors shown as scaled $\log_2$-fold changes (GEPIA data). **b** The mRNA expression levels of *CD274, CD276, VTCN1*, and *C10orf54* in human OvCa tumor tissues and normal ovarian tissues. The data were derived from the TCGA database, and are shown on a $\log_2(\text{TPM}+1)$ scale. TPM: transcripts per million. The *P*-value cutoff was 0.01. **c** Representative immunofluorescence images of PD-L1, B7-H3, B7S1, and VISTA in human OvCa and normal ovarian tissues. Original magnification ×40; scale bar, 50 μm. Inset original magnification ×100; scale bar, 25 μm. **d** Quantification of PD-L1$^+$, B7-H3$^+$, B7S1$^+$, and VISTA$^+$ cells in tumor and normal tissues (cell numbers were quantified in images of a ×100 field). Each dot represents the data from one patient. One-way ANOVA followed by Tukey's multiple comparison test. **e** Representative figures and summarized data showing the percentages of B7-H3-positive mDCs, DCs, Mø/Mo, and mMDSCs in tumors, ascites, and PBMCs from OvCa patients. One-way ANOVA followed by Tukey's multiple comparison test. The data are presented as the mean ± SEM; ns $P > 0.05$, *$P < 0.05$, **$P < 0.01$, ***$P < 0.0001$, and ****$P < 0.00001$

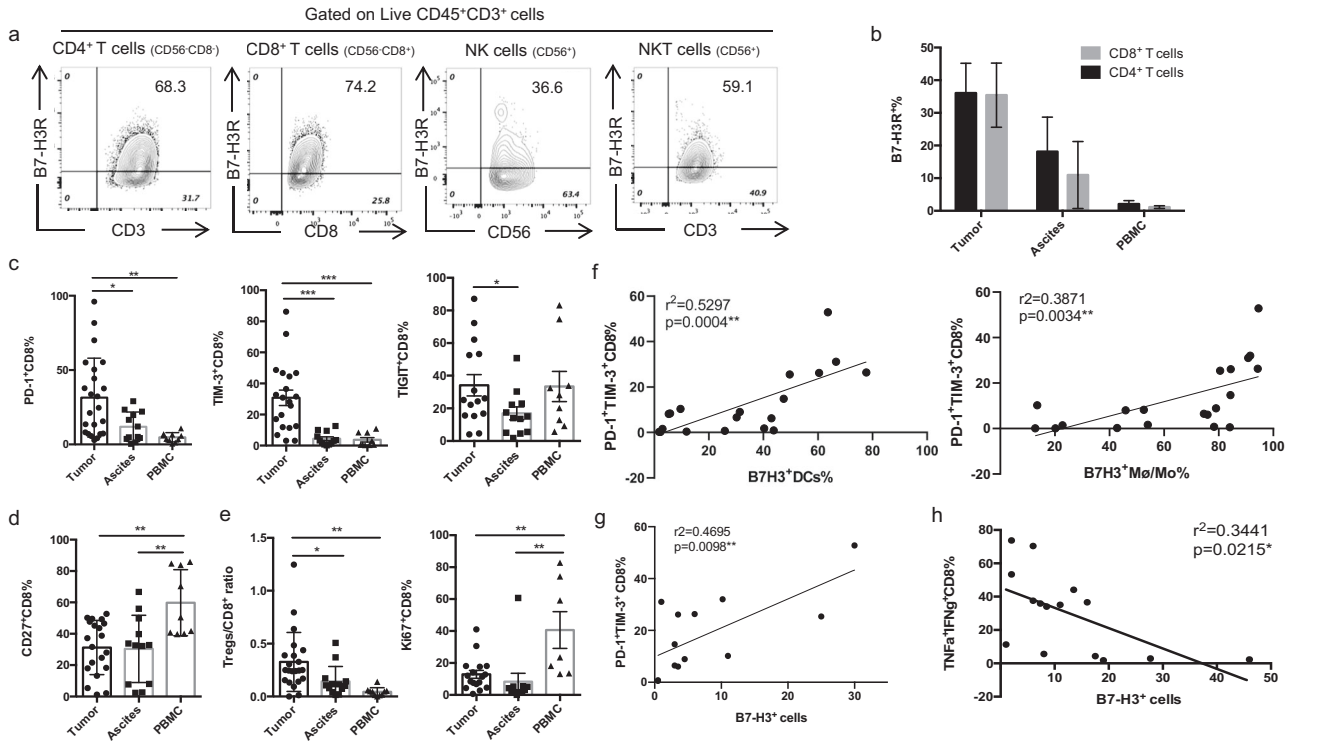

Fig. 2 High levels of B7-H3 expression in human OvCa are associated with CD8$^+$ TIL exhaustion. **a** Representative figures of B7-H3R expression on CD4$^+$ T cells, CD8$^+$ T cells, NK cells, and NKT cells in OvCa tumors detected by a biotinylated hB7-H3-mIgG2a Fc fusion protein. **b** Summary data for the percentages of B7-H3R$^+$ CD4$^+$ T cells and B7-H3R$^+$ CD8$^+$ T cells in tumors, ascites, and PBMCs. **c**, **d** Expression levels of coinhibitory molecules (PD-1, TIM-3, and TIGIT) (**c**) and the costimulatory molecule CD27 (**d**) on CD8$^+$ T cells from the tumors, ascites, and PBMCs of OvCa patients. **e** Ratio of Treg/CD8$^+$ T cells (left panel) and percentages of Ki67$^+$ CD8$^+$ T cells (right panel) in the tumors, ascites, and PBMCs of OvCa patients. **f** Correlations of the percentages of B7-H3$^+$ Mø/Mo (left panel) and B7-H3$^+$ DCs (right panel) with the percentage of PD-1$^+$ TIM-3$^+$CD8$^+$ TILs in human OvCa patients. **g**, **h** Association of B7-H3$^+$ cells in tumors with PD-1$^+$ TIM-3$^+$CD8$^+$ TILs (**g**) and TNF-α$^+$IFN-γ$^+$ CD8$^+$ TILs (**h**). The data are presented as the mean ± SEM. ns $P > 0.05$, *$P < 0.05$, **$P < 0.01$, and ***$P < 0.0001$. One-way ANOVA followed by Tukey's multiple comparison test was used in (**b**–**e**), and Spearman correlation analysis was performed for (**f**)

investigated the expression of the inhibitory receptors PD-1, TIM-3, and TIGIT and the costimulatory molecule CD27 on CD8$^+$ T cells isolated from the tumors, ascites, and PBMCs of OvCa patients. In the tumor tissue samples, the percentages of PD-1- and TIM-3-expressing CD8$^+$ T cells were significantly increased compared with those in the ascites and PBMCs (Fig. 2c; SI Appendix, Supplementary Fig. S2A, B). Similar increases were also observed for PD-1$^+$TIM-3$^+$CD8$^+$ and PD-1$^+$TIGIT$^+$CD8$^+$ T cells (SI Appendix, Supplementary Fig. S2C). Moreover, Fig. 2c shows that the frequencies of TIGIT$^+$CD8$^+$ T cells in the tumors were significantly higher than those in the ascites. In addition, the levels of CD27$^+$ CD8$^+$ T cells in the tumors were clearly decreased in comparison with those in the ascites and PBMCs (Fig. 2d; SI Appendix, Supplementary Fig. 2A and S2B). Consistently, Treg/CD8$^+$ T cell ratios were increased, and Ki67$^+$ CD8$^+$ T-cell frequencies were reduced in the tumors compared with the ascites and PBMCs (Fig. 2e).

The above data indicate that CD8$^+$ TILs from OvCa patients display the characteristic exhausted T-cell phenotype of PD-1, TIM-3, and TIGIT expression with decreased CD27 and Ki-67 expression. Correlation analysis revealed that on CD8$^+$ T cells, the expression levels of PD-1 positively correlated with those of TIM-3 and TIGIT, but negatively correlated with those of CD27 in the OvCa TME (SI Appendix, Supplementary Fig. S2D), suggesting that in human OvCa, PD-1 expression levels inversely correlate with T-cell function, which is consistent with previous papers.[1,38] Since B7-H3 was highly expressed in the TME (Fig. 1c–e), we assessed whether B7-H3 regulates T-cell exhaustion in human OvCa. Correlation analysis between B7-H3-expressing APCs and PD-1$^+$TiM-3$^+$ CD8$^+$ TILs showed that the frequency of PD-1$^+$ TIM-3$^+$ CD8$^+$ TILs positively correlated with the frequencies of B7-H3$^+$ Mø/Mo and B7-H3$^+$ DCs in the tumors (Fig. 2f). As B7-H3 is also expressed on CD45$^-$ cells, B7-H3$^+$ cells were quantified in immunofluorescence images of tumors in a ×100 field. The percentages of B7-H3$^+$ cells in the tumors also positively correlated with the frequencies of PD-1$^+$ CD8$^+$ TILs (Fig. 2g), but negatively correlated with the frequencies of TNF-α$^+$IFN-γ$^+$ CD8$^+$ T cells (Fig. 2h). These data strongly suggest that B7-H3 may regulate CD8$^+$ T-cell exhaustion in OvCa patients.

B7-H3 on tumor cells suppresses antitumor immunity in an ID8 mouse model

To analyze the function of B7-H3 in antitumor immunity, we generated *Cd276* knockout (KO) mice on the C57BL/6 background. The knockout vector was designed to remove exons 3–4 in the *Cd276* gene to create a null allele. Correct targeting of the *Cd276* locus was confirmed by southern blot analysis. *Cd276*$^{-/-}$ mice were born at the expected Mendelian frequencies and achieved a normal size, maturation, and fertility. We subcutaneously or intraperitoneally injected mouse OvCa ID8 cells undergoing logarithmic growth into wild-type (WT) and *Cd276*$^{-/-}$ mice. Unlike what we had previously observed with melanoma and hematopoietic tumors,[29] ID8 tumors did not show altered growth in the *Cd276*-deficient mice (Fig. 3a), and the *Cd276*-deficient mice did not show improved survival compared with the WT mice (Fig. 3b). These results indicate that B7-H3 expressed in host cells may not be functionally significant in the ID8 model.

Since B7-H3 was detected on tumor cells in addition to CD45$^+$ cells in human OvCa specimens, we next evaluated the expression of B7-H3 on ID8 cells using an antibody (clone 27-1) generated

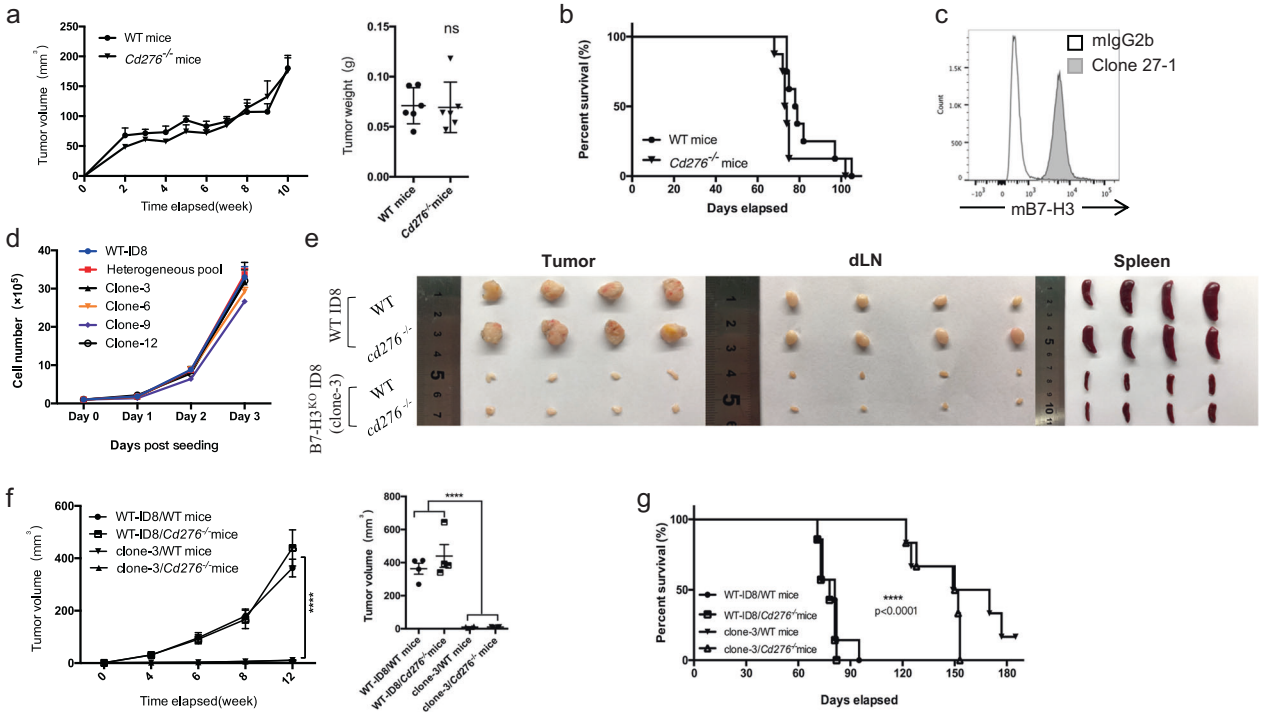

Fig. 3 B7-H3 deficiency in ID8 tumor cells suppresses tumor growth in tumor-bearing mice. **a** Tumor growth and tumor weight (week 10) in WT or *Cd276*$^{-/-}$ mice ($n = 6$) subcutaneously injected with 2×10^6 WT-ID8 cells. **b** Survival rates of WT mice and *Cd276*$^{-/-}$ mice injected with 2×10^6 WT-ID8 intraperitoneally. **c** Expression of B7-H3 on WT-ID8 cells. **d** Growth curves of WT-ID8 cells, B7-H3^{KO} ID8 clones, and the clone pool. **e**, **f** Representative images of tumors, draining lymph nodes, and spleens from tumor-bearing mice collected at week 12 (**e**). Tumor growth and mean tumor volume of subcutaneous WT-ID8 or B7-H3^{KO}-ID8 tumors in WT mice versus *Cd276*$^{-/-}$ mice ($n = 4$) (**f**). **g** Survival of WT and *Cd276*$^{-/-}$ mice ($n = 6$) injected with 2×10^6 WT-ID8 or B7-H3^{KO}-ID8 cells intraperitoneally. These experiments were repeated three times. The data are presented as the mean ± SEM. ns $P > 0.05$, *$P < 0.05$, **$P < 0.01$, and ***$P < 0.0001$. The *P*-values for tumor growth were determined by two-way ANOVA, those for tumor weight were determined by an unpaired *t* test, and those for survival were determined by the log-rank test

against the human B7-H3 protein that cross-reacted with mouse B7-H3 (SI Appendix, Fig. 3a). Consistent with the results for the human OvCa cell lines, B7-H3 was highly expressed on ID8 cells (Fig. 3c), while PD-L1 was expressed at a low baseline level (SI Appendix, Fig. 3b). To examine the role of B7-H3 expressed by ID8 cells in tumor progression, we used a guide RNA[39] targeting exon 3 of the *Cd276* gene and CRISPR/Cas9 to induce mutations in *Cd276* to generate B7-H3-deficient ID8 cells (B7-H3^{KO} ID8). To generate single-cell clones, the targeted cells were sorted by flow cytometry using an mCherry reporter, followed by limited dilution cloning. The loss of B7-H3 expression on the single clones was verified by antibody staining (SI Appendix, Supplementary Fig. S3C). B7-H3 deletion did not affect the morphology or proliferation of the ID8 cells in vitro (Fig. 3d). However, compared with WT-ID8 tumor-bearing mice, B7-H3^{KO} ID8 (clone 3) tumor-bearing WT and *Cd276*$^{-/-}$ mice showed significantly decreased tumor growth with a reduced tumor burden, diminished tumor-induced lymphadenectasis, and splenomegaly (Fig. 3e, f), and an increased survival rate (Fig. 3g) in both subcutaneous and intraperitoneal tumor models. Notably, there were no differences between the B7-H3^{KO} ID8 tumor-bearing WT mice and B7-H3^{KO} ID8 tumor-bearing *Cd276*$^{-/-}$ mice, indicating the dominant role of tumor-expressed B7-H3 in the ID8 model.

To exclude the possibility of clone-specific defects, we s.c. injected WT-ID8 cells, a pool of unsorted B7-H3^{KO} ID8 cells (a mixture of B7-H3^{+} and B7-H3^{-} ID8 cells) or four validated knockout clones (clones 3, 6, 9, and 12) into WT mice. Consistent with the above results for clone 3, B7-H3 deficiency in ID8 cells resulted in significantly reduced tumor progression, and even the clone 9-injected mice showed no tumor burden (SI Appendix, Supplementary Fig. S3D). Notably, there were no significant differences between clone 9 and the other clones in terms of an in vitro assay. Furthermore, the tumor growth in the mice injected with the unsorted B7-H3^{KO} ID8 pool was faster than that in the mice injected with the knockout clones, but slower than that in the mice injected with WT cells (SI Appendix, Supplementary Fig. S3D), which confirmed that B7-H3 deficiency in ID8 cells suppresses tumor progression. Together, these results indicate that B7-H3 expression on tumor cells accounts for most, if not all, of the function of promoting tumor growth in the ID8 OvCa model.

ID8-expressed B7-H3 inhibits T-cell effector functions

To elucidate the functional mechanisms involving B7-H3 in antitumor immunity, we i.p. injected WT-ID8 or B7-H3^{KO} ID8 (clone 3) cells into WT mice and compared the phenotypes of the T cells in the ascites or peritoneal lavage fluid at 8 weeks. Compared with those isolated from the WT-ID tumor-bearing mice, CD8^{+} TILs isolated from the B7-H3^{KO}-ID8 tumor-bearing mice displayed decreased expression of the coinhibitory molecule PD-1 (Fig. 4a), but increased surface expression of the degranulation maker CD107a and the proliferation marker Ki67 (Fig. 4b; SI Appendix, Supplementary Fig. S4A) and produced increased levels of IFN-γ, TNF-α, and granzyme B upon PMA/ionomycin stimulation (Fig. 4c; SI Appendix, Supplementary Fig. S4A). However, the percentages of CD8^{+} TILs were decreased in the B7-H3^{KO} group, probably due to the reduced tumor burden in these mice (SI Appendix, Supplementary Fig. S4B). We also analyzed the phenotypes of CD4^{+} T cells and NK cells in the TME and found increased frequencies of tumor-infiltrating CD4^{+} T cells and NK cells expressing TNF-α and IFN-γ in the mice challenged with B7-H3^{KO}-ID8 cells (SI Appendix, Supplementary Fig. S4C), although

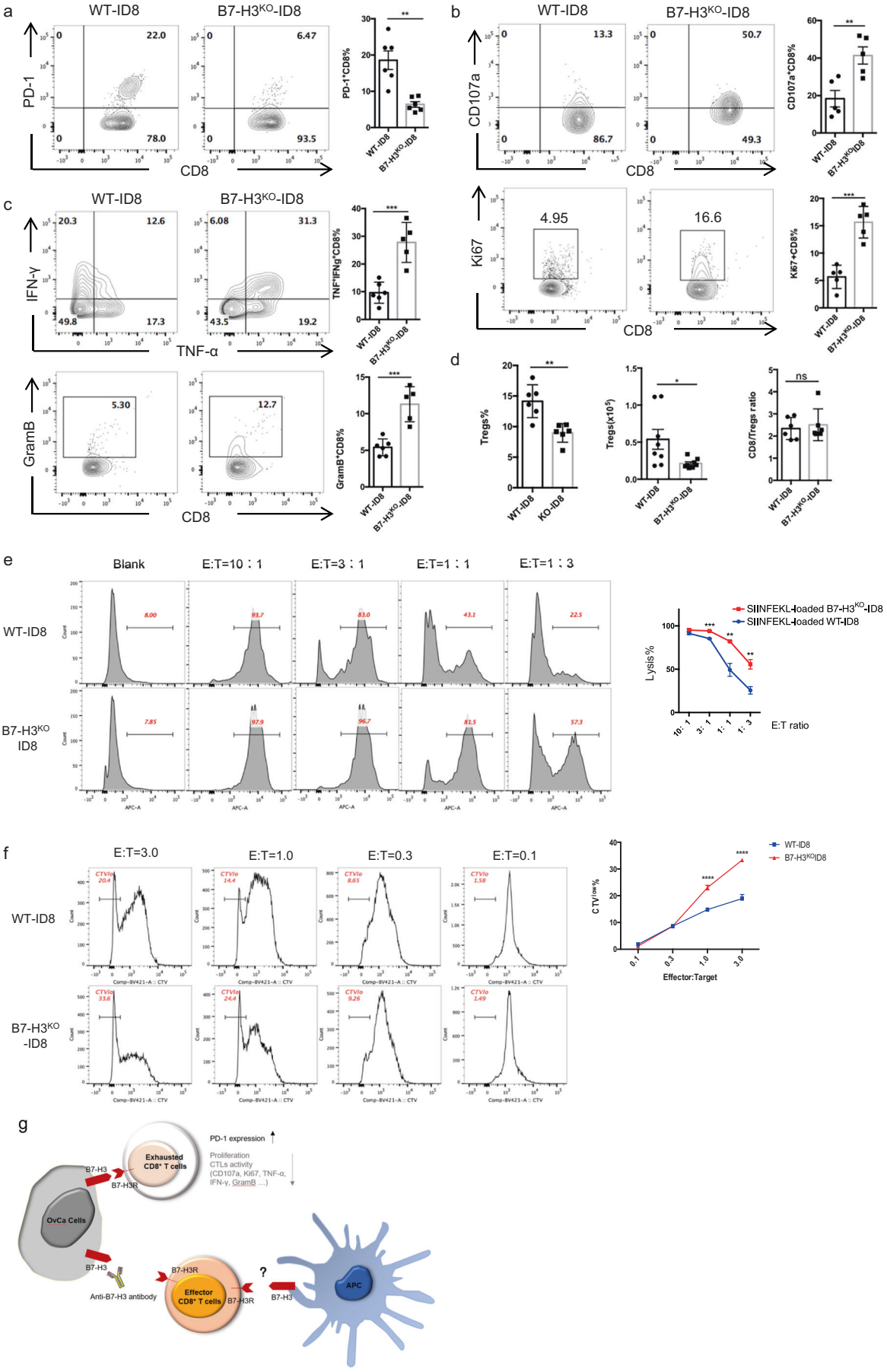
a
WT-ID8
B7-H3KO-ID8
PD-1
CD8
22.0
78.0
6.47
93.5
PD-1+CD8%
b
CD107a
13.3
86.7
50.7
49.3
CD107a+CD8%
c
IFN-γ
TNF-α
20.3
49.8
12.6
17.3
6.08
43.5
31.3
19.2
TNF+IFNg+CD8%
Ki67
4.95
16.6
Ki67+CD8%
GramB
5.30
12.7
GramB+CD8%
d
Tregs%
Tregs(x10⁵)
CD8/Tregs ratio
KO-ID8
ns
e
Blank
E:T=10：1
E:T=3：1
E:T=1：1
E:T=1：3
WT-ID8
B7-H3KO ID8
8.00
93.7
83.0
43.1
22.5
7.85
97.9
96.7
81.5
57.3
SIINFEKL-loaded B7-H3KO-ID8
SIINFEKL-loaded WT-ID8
Lysis%
E:T ratio
f
E:T=3.0
E:T=1.0
E:T=0.3
E:T=0.1
WT-ID8
B7-H3KO -ID8
CTV low %
Effector:Target
g
PD-1 expression
Proliferation
CTLs activity
(CD107a, Ki67, TNF-α,
IFN-γ, GramB …)
Exhausted CD8+ T cells
B7-H3
B7-H3R
OvCa Cells
Anti-B7-H3 antibody
Effector CD8+ T cells
APC

Fig. 4 B7-H3 on ID8 cells induces dysfunction in $CD8^+$ TILs. **a** Representative figures and summarized data showing PD-1 expression on $CD8^+$ TILs. **b** Representative figures and summarized data showing the baseline expression of CD107a (upper panel) and Ki-67 (bottom panel) on $CD8^+$ T cells in ascites or peritoneal lavage fluid from mice injected with 2×10^6 WT or B7-$H3^{KO}$-ID8 cells. **c** Representative figures and summarized data showing the expression of granzyme B, TNF-α, and IFN-γ after PMA and ionomycin stimulation. **d** Percentages and absolute cell numbers of Tregs and the ratio of $CD8^+$ T cells to Tregs. **e** Representative figures and summarized data showing cytolysis of WT or B7-$H3^{KO}$-ID8 cells, effector cells, OT-1 T cells, target cells, WT, or B7-$H3^{KO}$-ID8 cells. **f** Representative figures and summarized data showing the proliferation rate of OT-1 T cells after coculture with WT or B7-$H3^{KO}$-ID8 cells. Schematic diagram of how B7-H3 regulates antitumor immunity in OvCa. These experiments were repeated three times with similar data. Mean ± SEM; unpaired *t* test; $^*P < 0.05$, $^{**}P < 0.01$, $^{***}P < 0.0001$, and $^{****}P < 0.00001$

there was no difference in CD107a expression (SI Appendix, Supplementary Fig. S4D). Moreover, B7-H3 deficiency in ID8 cells significantly reduced Treg cell infiltration in terms of both percentages and absolute cell numbers, although the $CD8^+$/Treg cell ratio was not difference between the two groups (Fig. 4d). These results demonstrate that B7-H3 expressed on ID8 cells inhibits antitumor immunity and promotes T-cell exhaustion.

To confirm the regulation of $CD8^+$ T-cell functions by B7-H3, we next conducted an in vitro cytotoxicity assay in which we first activated OT-1 T cells with $OVA_{257–264}$ (SIINFEKL)-loaded splenic APCs for 4 days and then cocultured them with SIINFEKL-loaded WT-ID8 cells or B7-$H3^{KO}$ ID8 cells at different E/T ratios for 5 h. Enhanced levels of target cell lysis were observed with the B7-$H3^{KO}$-ID8 cells compared with the WT-ID8 cells, and target cell lysis appeared to be dose dependent (Fig. 4e). Furthermore, B7-H3 deficiency in ID8 cells resulted in increased TNF-α and IFN-γ secretion by $CD8^+$ T cells (SI Appendix, Supplementary Fig. S4E), indicating that B7-H3 on ID8 cells inhibits CTL functions. To test whether B7-H3 on tumor cells affects T-cell proliferation, we cocultured SIINFEKL-loaded WT or B7-$H3^{KO}$ ID8 cells with CTV-labeled naive OT-1 T cells for 4 days; the B7-$H3^{KO}$ ID8 cells increased proliferation by the OT-1 T cells (Fig. 4f). Collectively, these data indicate that tumor-intrinsic B7-H3 promotes tumor development by inhibiting the expansion and cytotoxic functions of effector $CD8^+$ T cells in the TME (Fig. 4g).

Therapeutic targeting of B7-H3 promotes survival in the ID8 model

The above results showed that deficiency in B7-H3 in ID8 cells enhanced tumor cell immunogenicity and promoted the functions of $CD8^+$ T cells. To address whether B7-H3 can serve as a target for immunotherapy in OvCa, we monitored tumor growth in a therapeutic setting. WT mice were first intraperitoneally inoculated with WT-ID8 cells, and subsequently treated with an anti-IgG, anti-B7-H3, anti-PD-1, or anti-B7-H3 antibody plus an anti-PD-1 antibody injected i.p. on days 30, 32, 34, 36, and 38 (Fig. 5a). The ID8 tumor-bearing mice failed to respond to anti-PD-1 treatment, which was consistent with previous reports.[20–23] In contrast, the tumor-bearing mice treated with the anti-B7-H3 antibody alone or combined with the anti-PD-1 antibody exhibited prolonged survival compared with those given control treatment or anti-PD-1 antibody treatment alone, and the median survival was increased from 80 (the anti-PD-1 group) or 82 days (the control IgG group) to 93.5 (the anti-B7-H3 group) and 95 days (the combination group) (Fig. 5b). However, the anti-B7-H3 and anti-PD-1 combinatorial treatment did not show any synergistic effects (Fig. 5b), demonstrating that in the ID8 OvCa model, immunotherapeutic targeting of the B7-H3 pathway may potently elicit antitumor immune responses in a PD-1-independent fashion.

DISCUSSION

Despite rapid progress in immunotherapy, particularly the landslide approval of PD-L1/PD-1 blockade therapies for many types of tumors, OvCa remains generally resistant.[9] In our study, we found that B7-H3, but not PD-L1, was highly expressed in OvCa, which positively correlated with $CD8^+$ T-cell exhaustion. B7-H3, expressed on tumor cells but not APCs, regulated progression in the mouse ID8 OvCa model by attenuating the expansion and cytotoxicity of $CD8^+$ T cells. Therapeutically, blockade of B7-H3 but not PD-1 prolonged survival in the ID8 OvCa model, highlighting B7-H3 as a potential target in patients resistant to the PD-L1/PD-1 blockade therapy.

PD-L1/PD-1 blockade elicits potent and durable antitumor effects, especially on some refractory tumors.[5,40] However, in clinical practice, only a small patient population (<30%) benefits from these treatments, while nonresponders undergo transient reinvigoration of exhausted T cells followed by disease relapse.[41] As the most widely used predictor, the expression levels of PD-L1 are positively associated with the overall response rates to anti-PD-L1/PD-1 immunotherapies,[3] although it is still controversial whether the expression of PD-L1 on tumor cells or immune cells affects the response rates.[5] We found that in human OvCa, PD-L1 mRNA expression was low, with no obvious difference from the expression in normal ovarian tissue. The immunofluorescence data showed that, at the protein level, PD-L1 was upregulated at tumor sites compared with normal tissue sites, and the majority of PD-L1 expression was observed on pancytokeratin-negative cells, especially professional APCs (Mø/Mo and DCs). However, the flow-cytometry data showed that, on $CD45^+$ cells isolated from OvCa patients, <5% of tumor-infiltrating APCs on average expressed PD-L1, which was not significantly different from the percentages in ascites and PBMCs from OvCa patients. Moreover, human OvCa cell lines and isolated primary OvCa cells expressed PD-L1 at a low or undetectable level, which was consistent with the immunofluorescence data and reported data.[35] Since IFN-γ has been reported to upregulate PD-L1 expression on human OvCa cells,[35] the expression of PD-L1 was directly tested by flow cytometry once primary cells were isolated from OvCa specimens. The low level of PD-L1 expression on the primary cells isolated from OvCa could not be explained by nonexposure to an IFN-γ-rich TME. As high PD-L1 expression levels are related to increased response rates and clinical benefits in anti-PD-L1/PD-1 therapies,[3] the poor expression of PD-L1 by tumor and immune cells may contribute to the low ORR of OvCa patients to PD-L1/PD-1 blockade.

High expression of B7-H3 in tumors has been described,[26–28] and the overexpression of B7-H3 has been reported to be associated with a reduced number of TILs,[42] a poor prognosis, and poor clinical outcomes.[32] High expression of B7-H3 in OvCa has been reported at the tissue level.[33] In our study, we further demonstrated robust expression of B7-H3 in human OvCa. In addition, we also found that the expression of B7-H3 in the OvCa TME was higher than that of other family members, specifically PD-L1, B7S1, and VISTA, at both the mRNA and protein levels. According to the reported data, in OvCa, B7-H3 is mainly expressed on tumor cells,[35] while lymphocytes are B7-H3 negative.[28] However, in our study, we showed that B7-H3 was broadly expressed in the OvCa TME. In addition to being expressed on CD45-negative cells, B7-H3 was also found to be highly expressed on CD45-positive cells. We found that among $CD45^+$ cells, tumor-infiltrating APCs, including mDCs, Mø/Mo, and mMDSCs, were the major B7-H3-positive population, while in ascites, B7-H3 was predominantly expressed on tumor-associated Mø/Mo. In addition, B7-H3 expression in the TME of OvCa positively correlated with the frequency of PD-1^+ TIM-3^+ $CD8^+$ T cells and negatively correlated with the frequency of TNF-α^+ IFN-γ^+ $CD8^+$ T cells, while a putative receptor of B7-H3 was

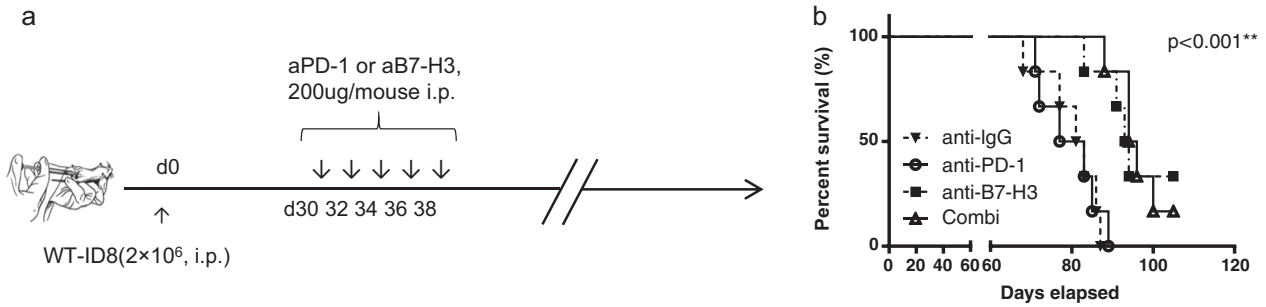

Fig. 5 Blockade of B7-H3 prolongs survival in the ID8 model. **a** Experimental protocol for ID8 challenge in mice followed by treatment via intraperitoneal injection of a control ab, an anti-B7-H3 mAb, an anti-PD-1 mAb, or the anti-B7-H3 mAb plus the anti-PD-1 mAb (combo). **b** Survival curves of the WT-ID8-bearing mice treated with the blocking antibodies ($n = 6$); log-rank test, $^{**}P < 0.01$

detected on $CD8^+$ TILs. Thus, B7-H3 may promote $CD8^+$ T-cell exhaustion in OvCa.

B7-H3 expressed by APCs has been reported to potently inhibit T and NK cell activation, and anti-B7-H3 treatment significantly reduces tumor growth in E.G7 and MOPC315 mouse models.[29] In a previous study, B7-H3 on APCs but not on tumor cells was found to account for tumor immune escape. However, in our study, we found that in the ID8 model, *Cd276*$^{-/-}$ mice showed no significant change in tumor growth compared with WT mice. Similar phenomena have also been observed in MC38 colon tumor-, SW620 colon tumor-, and UACC melanoma-bearing mice.[39] Interestingly, deletion of *Cd276* in ID8 cells delayed tumor growth and extended survival. Notably, B7-H3^{KO} ID8 tumor-bearing *Cd276*$^{-/-}$ mice had tumor growth and survival curves similar to those of WT mice injected with the same tumor cells. These data indicate that in the ID8 model, tumor-expressed B7-H3 plays a predominant role. Furthermore, consistent with human OvCa, a murine model of OvCa showed that the PD-L1/PD-1 pathway blockade alone had little therapeutic effect.[20–23] In line with that finding, we found no obvious effect of anti-PD-1 treatment on survival, whereas anti-B7-H3 treatment significantly increased overall survival in mice. In addition, although dual blockade of PD-1 with B7-H3 has been shown to enhance the strength of immunotherapeutic effects on the E.G7 and MOPC315 models,[29] a combined anti-B7-H3 and anti-PD-1 treatment did not show synergistic effects on the ID8 model. Taken together, the findings indicate that B7-H3 expressed on both tumor-infiltrating APCs and tumor cells can play a critical role in suppressing antitumor immunity and that the contribution of B7-H3 in the TME is context dependent, which requires further exploration. Tumor-expressed B7-H3 induces PD-1-independent suppression of antitumor immune responses in the ID8 model, but whether dual blockade of PD-1 and B7-H3 in human OvCa patients has synergistic effects remains unknown.

In addition to its immunoregulatory roles, OvCa cell-expressed B7-H3 has also been reported to promote tumor cell invasion and migration by influencing the jak2-Stat3 pathway and has been associated with distant metastasis.[43] Interruption of metastatic pathways holds preclinical and clinical promise as an antimetastasis therapy.[44] Therefore, targeting B7-H3 may also be a promising way to treat advanced metastatic OvCa. However, since OvCa also expresses B7S1 and VISTA in the TME, whether B7-H3 predominates over those molecules remains to be investigated.

In conclusion, our study shows an important role for B7-H3, but not PD-L1 in OvCa. B7-H3 may serve as a promising target in cancer patients resistant to the PD-L1/PD-1 blockade therapy, including OvCa patients. Our work also calls for detailed characterization of the TME in terms of the expression of checkpoint molecules in addition to PD-L1 to offer precise and personalized immunotherapy for a variety of cancers.

MATERIALS AND METHODS

Patients and specimens

Fresh tumor tissues, malignant ascites, and matched blood were collected from OvCa patients undergoing primary surgical treatment without chemotherapy at Shanghai First Maternity and Infant Hospital. All the experimental protocols were approved by the institutional review committee.

Isolation of PBMCs and tumor-infiltrating lymphocytes from tumors or ascites

Blood and ascites from OvCa patients were collected into heparinized tubes and centrifuged on Ficoll-Hypaque gradients (GE Healthcare Life Sciences). Fresh tumors from OvCa patients were digested in the RPMI-1640 medium supplemented with 1 mg/mL Collagenase A (Gibco) for 30 min at 37 °C prior to Ficoll-Hypaque gradient centrifugation.

Mice

Six- to eight-week-old female mice were used for all experiments. C57BL/6J mice, *Cd276*$^{-/-}$ mice (on the C57BL/6J background) and OT-1 mice were bred and housed under specific pathogen-free conditions in the Animal Facility of Tsinghua University and used in accordance with the animal care guidelines from the National Institutes of Health. Animal protocols were reviewed and approved in accordance with governmental and institutional guidelines for animal welfare.

Generation of Cd276$^{-/-}$ mice

Mice were generated according to a service contract with Biocytogen, Beijing, China. Specifically, exons 3 and 4 of *Cd276*, which encode the extracellular domain of the B7-H3 protein, were chosen for targeting. A pair of loxP sites and a Frt-Neo-Frt-loxp cassette were designed to be inserted into intron 2 and intron 4, respectively. The targeting vector was linearized and electroporated into embryonic stem (ES) cells, followed by G418 selection. Targeted ES clones were identified by southern blot hybridization analysis by using a 5′ probe, 3′ probes, and Neo-probe. The targeted ES clones were then microinjected into BALB/c blastocysts, and F1 chimeric mice (*Cd276*fl-neo/+) were generated. *Cd276*fl-neo/+ mice were bred with Flp-deleter mice to generate *Cd276*fl/+, Flp/+ mice, and *Cd276*fl/+ mice were crossed with Cre-deleter mice to generate *Cd276*$^{-/-}$ mice. The following three primers were designed for genotyping: F 5′-GTTCTGCAGGCACCCTTCCTAT-3′, R1 5′-CCAAG ACCCAGGTCATACCCTG-3′, and R2 5′-CAGTTGAGTGAGATGCA CCTTC-3′. The primers F and R1 amplified the wild-type allele (348 bp), and the primers F and R2 amplified the null allele (372 bp).

The *Cd276*$^{-/-}$ mice were generated under a service contract with Biocytogen, Beijing, China.

Cell lines

Mouse ID8 cells (a gift from Dr. Xueguang Zhang, Soochow University, China) and the human OvCa cell lines HeyA8, Hey, OVC429, OVCA433 (gifts from Fudan University Shanghai Cancer Center), A2780, SKOV3, and H08910-PM (purchased from ATCC) were cultured in vitro in Dulbecco's Modified Eagle Medium (DMEM) supplemented with 10% FBS (Gibco) and 100 IU/ml Penicillin/Streptomycin (Corning).

To generate stable B7-H3^{KO} ID8 cells, a guide RNA (gRNA) targeting mouse B7-H3 (TGGCACAGCTCAACCTCATC) was inserted into the vector LentiCRISPR v2-mCherry[45]. HEK293T cells were cotransfected with the plasmids pLectiCRISPR-mCherry-gRNA, pMD2.G (Addgene, 12259), and psPAX2 (Addgene, 12260) by PEI Max to produce a lentivirus. The lentivirus was employed to infect the mouse ovarian cancer cell line ID8. Forty-eight hours after infection, the mCherry-positive cells were sorted and subcloned to generate single-cell clones. To verify the mB7H3$^{-/-}$ cell clones, the single-cell clones were stained with an antibody generated against the human B7-H3 protein that cross-reacted with mouse B7-H3 (clone 27–1) (Suzhou Kanova Biopharmaceutical Co., Ltd.), followed by a PE-conjugated goat anti-mouse IgG secondary antibody, and DNA sequencing was conducted for further confirmation. All cell lines tested negative for mycoplasma contamination.

Murine tumor models

Female C57BL/6J mice and *cd276*$^{-/-}$ mice were inoculated subcutaneously or intraperitoneally with 2×10^6 WT-ID8 or B7-H3$^{-/-}$ ID8 cells. Tumor growth in the s.c. model was measured with Vernier calipers every week, and tumor volume was calculated as $0.5 \times \text{length} \times \text{width}^2$. The mice were killed after 8 (i.p.) or 12 (s.c.) weeks for phenotypic analyses. To test the therapeutic effects of an anti-B7-H3 mAb (clone 110, produced in high quantities by BioXcell, NH, USA) and the combinatorial blockade of B7-H3 and PD-1, female C57BL/6J mice were i.p. inoculated with 2×10^6 WT-ID8 cells and then treated with 200 μg control rat IgG, 200 μg anti-B7-H3 mAb (clone 110, BioXcell, NH, USA), 200 μg anti-PD-1 mAb (clone J43, BioXcell, NH, USA), or 200 μg anti-B7-H3 mAb (clone 110, BioXcell, NH, USA) plus 200 μg anti-PD-1 mAb (clone J43, BioXcell, NH, USA) on days 30, 32, 34, 36, and 38. Survival time points were based on reaching a cutoff weight of 35 g as a result of ascites accumulation.

Flow cytometry

For human specimens, the following fluorescent dye-conjugated antibodies were used: anti-CD45-PerCP-CY5.5 (HI30, BioLegend), anti-Lineage-FITC (UCHT1, HCD14, 3G8, HIB19, 2H7, and HCD56, BioLegend), anti-HLA-DR-AF700 (L243, BioLegend), anti-CD11c-BV605 (3.9, BioLegend), anti-CD123-PE-CF594 (7G3, BioLegend), anti-CD14-APC-CY7 (M4P9, BioLegend), anti-CD15-PE-CY5 (W6D3, BioLegend), anti-B7-H3-PE (DCN.70, BioLegend), anti-B7S1-PE-CY7 (MIH43, BioLegend), anti-VISTA (730804, R&D), Streptavidin-BV421 (BioLegend), anti-PD-L1-APC (MIH1, BD), anti-CD3-PerCP-CY5.5 (OKT3, BioLegend), anti-CD56-FITC (HCD56, BioLegend), anti-CD4-PE-CF594 (L200, BD), anti-CD8-AF700 (SK1, BD), anti-FoxP3-PE-CF594 (259D/C7, BD), anti-TIM-3-PE (F38-2E2, BioLegend), anti-TIGIT-PerCP-eFluor 710 (MBSA43, eBioscience), anti-CD27-PerCP-CY5.5 (O323, BioLegend), anti-PD-1-PE (EH12.2H7, BioLegend), anti-Ki-67-AF700 (B56, BD), anti-TNF-α-PE-CF594 (Mab11, BioLegend) and anti-IFN-γ-PE-CY7 (B27, BioLegend). The following antibodies were used in animal model experiments: anti-CD45.2-APC-CY7(BioLegend) or PE (104, eBioscience), anti-CD3e-PE or PE-CY7 (145-2C11, eBioscience), anti-NK-1.1-PerCP-CY5.5 (PK136, eBioscience), anti-CD4-PE-CF594 (RM4–5, BD), anti-CD8α-AF700 or APC (53–6.7, eBioscience), anti-PD-1-PE (J43, eBioscience), anti-Granzyme B-APC (NGZB, eBioscience), anti-Perforin-FITC (ebio-omakd, eBioscience), anti-Foxp3-eFluor 450 (FJK-16 s, eBioscience), anti-IFN-γ-eFluor 450 (XMG1.2, eBioscience), anti-TNF-α-PE-CY7 (MP6-XT22, BD), and anti-CD107a-Pacific Blue (1D4B, BioLegend). Single-cell suspensions were prepared as indicated. Dead cells were excluded by viability dye staining (fixable viability dye eF506, eBioscience). Surface immunofluorescence staining was performed at 4 °C for 20 min. For intracellular cytokine staining, cells were stimulated with PMA (50 ng/ml, Sigma-Aldrich, MO)/ionomycin (500 ng/ml, Sigma-Aldrich, MO) in the presence of Brefeldin A (Golgi-plug, BD Bioscience) for 4 h. After stimulation, the cells were stained for surface markers, fixed and permeabilized with the eBioscience fixation/permeabilization buffer, and then stained with antibodies at 4 °C for 40 min. To detect the expression of the human B7-H3 receptor and mouse B7-H3, a cell suspension was incubated with 10 μg/ml biotinylated human B7-H3-mIgG2a Fc fusion protein (generated in-house, N/A) or 10 μg/ml biotinylated anti-mouse B7-H3 antibody (clone 27-1, Suzhou Kanova Biopharmaceutical Co., Ltd.) at 4 °C for 40 min and then incubated with 0.5 μg/ml streptavidin-Brilliant Violet 421 (BioLegend) together with surface antibodies. Cells were acquired by an LSRFortessa (BD) flow cytometer, and data were analyzed using FlowJo X software.

Immunofluorescence

Paraffin sections of human OvCa specimens were dewaxed in xylene, dehydrated in ethanol, subjected to heat-induced epitope retrieval, and incubated with primary antibodies against human CD45 (ab10559), B7-H3 (6A1, ab105922), PD-L1 (ab55810), PD-1 (NAT105, ab52587), B7-S1 (MIH43, ab110221), VISTA (MAB71261), and Pancytokeratin (SC-15367) at 4 °C overnight. AffiniPure F(ab')2 Fragment donkey anti-rabbit immunoglobulin (Jackson Immuno Research, 711-546-152), AffiniPure F(ab')2 Fragment donkey anti-mouse immunoglobulin (Jackson Immuno Research, 715-166-150), and AffiniPure F(ab')2 Fragment donkey anti-goat (Jackson Immuno Research, 705-606-147) immunoglobulin antibodies were chosen as the secondary antibodies. All slides were incubated with mounting medium containing DAPI for 20 min. Images were obtained by using a Zeiss fluorescence microscope. Quantification analysis was performed by using ImageJ software.

ELISA

Human or mouse B7-H3 protein (2 μg/ml) was used to coat Nunc MaxiSorp™ flat-bottom 96-well ELISA Plates (eBioscience) at 4 °C overnight. The wells were blocked with 2% BSA at RT for 1 h. Then, the cells were incubated with serial dilutions of an anti-B7-H3 antibody (clone 27-1) (Suzhou Kanova Biopharmaceutical Co., Ltd.) at room temperature for 2 h, followed by incubation with a goat anti-mouse IgG-HRP secondary antibody (EASYBIO) for 1 h. A 1 × TMB substrate solution (eBioscience) was added to the wells and incubated for several minutes. The reaction was stopped by adding a 2 N H_2SO_4 stop solution. The plate was read at 450 nm by an iMark Microplate reader (Bio-Rad). Between each incubation, the wells were washed with PBST at least three times.

In vitro cytotoxicity assay

Murine splenic APCs were isolated from the spleens of female C57BL/6 mice and stimulated with 10 ng/ml SIINFEKL peptide ($OVA_{257–264}$) at 37 °C for 1 h. The $OVA_{257–264}$-loaded splenic APCs were cocultured with $CD8^+$ T cells isolated from female OT-1 mice for 4 days. Activated OT-1 CTLs were collected with a Dynabeads Flowcomp mouse CD8 kit (Invitrogen) and used as effector cells, while CFSE-labeled WT-ID8 and B7-H3$^{-/-}$ ID8 cells were pulsed with 10 ng/ml $OVA_{257–264}$ and used as target cells. The target cells were cocultured with effector cells at various E/T ratios at 37 °C overnight. The percentage of dead cells in the $CFSE^+$ ID8 population and the cytokine secretion by $CD8^+$ OT-1 CTLs were measured by FCM. To explore the role of tumor-intrinsic B7-H3 in T-cell proliferation, SIINFEKL-loaded WT or B7-H3$^{-/-}$ ID8 cells were cocultured with CTV-labeled naive OT-1 T cells at different E/T ratios for 4 days, and CTV-negative ID8 cells were detected by FCM.

Statistics

Statistical analyses were conducted with Prism 6.0 software (GraphPad) using the appropriate test as indicated in the figure legends. All values are expressed as the mean ± SEM. *P*-values <0.05 were considered statistically significant.

ACKNOWLEDGEMENTS

The authors are grateful to Dr. Xueguang Zhang (Soochow University, China) and Jiajia Li (Fudan University Shanghai Cancer Center) for providing the mouse and human OvCa cell lines. This project was funded in part by the Key Program of the National Natural Science Foundation of China (81730039 & 81671460 to L.-P.J.), the National Key Research and Development Program of China (2017YFC1001401 to L.-P.J.), Beijing Municipal Science and Technology Projects (Z181100006318015 and Z181100001318007 to C.D.), Shanghai Municipal Medical and Health Discipline Construction Projects (2017ZZ02015 to L.-P.J.), and the National Basic Research Program of China (2015CB943300 to L.-P.J.).

AUTHOR CONTRIBUTIONS

D.C., L.N., L.J. and C.D. conceived and designed the study. D.C., J.L., D.L., S.H., Q.Q., Q.S., S.X. and T.S. conducted the experiments. P.L. and N.L. supervised and collected the clinical specimens. D.C. and J.L. analyzed and interpreted the data. L.G. and L.J. provided key materials. D.C., L.N. and C.D. wrote and revised the paper. L.J. and C.D. supervised the study.

ADDITIONAL INFORMATION

The online version of this article (https://doi.org/10.1038/s41423-019-0305-2) contains supplementary material.

Competing interests: The authors have filed a patent application based on the current work.

REFERENCES

1. Thommen, D. S. et al. A transcriptionally and functionally distinct PD-1(+) CD8(+) T cell pool with predictive potential in non-small-cell lung cancer treated with PD-1 blockade. *Nat. Med.* **24**, 994–1004 (2018).
2. Pardoll, D. M. The blockade of immune checkpoints in cancer immunotherapy. *Nat. Rev. Cancer* **12**, 252–264 (2012).
3. Mariathasan, S. et al. TGFbeta attenuates tumour response to PD-L1 blockade by contributing to exclusion of T cells. *Nature* **554**, 544–548 (2018).
4. Callahan, M. K., Postow, M. A. & Wolchok, J. D. Targeting T cell co-receptors for cancer therapy. *Immunity* **44**, 1069–1078 (2016).
5. Yi, M. et al. Biomarkers for predicting efficacy of PD-1/PD-L1 inhibitors. *Mol. Cancer* **17**, 129 (2018).
6. Patel, S. P. & Kurzrock, R. PD-L1 expression as a predictive biomarker in cancer immunotherapy. *Mol. Cancer Ther.* **14**, 847–856 (2015).
7. Motzer, R. J. et al. Nivolumab for metastatic renal cell carcinoma: results of a randomized phase II trial. *J. Clin. Oncol.* **33**, 1430–1437 (2015).
8. McDermott, D. F. et al. Atezolizumab, an anti-programmed death-ligand 1 antibody, in metastatic renal cell carcinoma: long-term safety, clinical activity, and immune correlates from a phase Ia study. *J. Clin. Oncol.* **34**, 833–842 (2016).
9. Song, M. et al. IRE1alpha-XBP1 controls T cell function in ovarian cancer by regulating mitochondrial activity. *Nature* **562**, 423–428 (2018).
10. Fan, C. A., Reader, J. & Roque, D. M. Review of Immune therapies targeting ovarian cancer. *Curr. Treat. Options Oncol.* **19**, 74 (2018).
11. Zhang, L. et al. Intratumoral T cells, recurrence, and survival in epithelial ovarian cancer. *N. Engl. J. Med.* **348**, 203–213 (2003).
12. Kandalaft, L. E., Powell, D. J. Jr., Singh, N. & Coukos, G. Immunotherapy for ovarian cancer: what's next? *J. Clin. Oncol.* **29**, 925–933 (2011).
13. Hamanishi, J. et al. Safety and antitumor activity of anti-PD-1 antibody, nivolumab, in patients with platinum-resistant ovarian cancer. *J. Clin. Oncol.* **33**, 4015–4022 (2015).
14. Hwang, W. T., Adams, S. F., Tahirovic, E., Hagemann, I. S. & Coukos, G. Prognostic significance of tumor-infiltrating T cells in ovarian cancer: a meta-analysis. *Gynecol. Oncol.* **124**, 192–198 (2012).
15. Hamanishi, J. et al. Programmed cell death 1 ligand 1 and tumor-infiltrating CD8+ T lymphocytes are prognostic factors of human ovarian cancer. *Proc. Natl Acad. Sci. USA* **104**, 3360–3365 (2007).
16. Brahmer, J. R. et al. Safety and activity of anti-PD-L1 antibody in patients with advanced cancer. *N. Engl. J. Med.* **366**, 2455–2465 (2012).
17. Ventriglia, J. et al. Immunotherapy in ovarian, endometrial and cervical cancer: State of the art and future perspectives. *Cancer Treat. Rev.* **59**, 109–116 (2017).
18. Disis ML, P. M. et al. Avelumab (MSB0010718C; anti- PD-L1) in patients with recurrent/refractory ovarian cancer from the JAVELIN solid tumor phase ib trial: safety and clinical activity. *J. Clin. Oncol.* **34**, 5533 (2016).
19. Varga, A. et al. Pembrolizumab in patients with programmed death ligand 1-positive advanced ovarian cancer: analysis of KEYNOTE-028. *Gynecol Oncol.* **152**, 243–250 (2019).
20. Guo, Z., Wang, H., Meng, F., Li, J. & Zhang, S. Combined trabectedin and anti-PD1 antibody produces a synergistic antitumor effect in a murine model of ovarian cancer. *J. Transl. Med.* **13**, 247 (2015).
21. Guo, Z. et al. PD-1 blockade and OX40 triggering synergistically protects against tumor growth in a murine model of ovarian cancer. *PLoS One* **9**, e89350 (2014).
22. Lu, L. et al. Combined PD-1 blockade and GITR triggering induce a potent anti-tumor immunity in murine cancer models and synergizes with chemotherapeutic drugs. *J. Transl. Med.* **12**, 36 (2014).
23. Peng, J. et al. Chemotherapy induces programmed cell death-ligand 1 overexpression via the nuclear factor-kappaB to foster an immunosuppressive tumor microenvironment in ovarian cancer. *Cancer Res.* **75**, 5034–5045 (2015).
24. Chapoval, A. I. et al. B7-H3: a costimulatory molecule for T cell activation and IFN-gamma production. *Nat. Immunol.* **2**, 269–274 (2001).
25. Sun, M. et al. Characterization of mouse and human B7-H3 genes. *J. Immunol.* **168**, 6294–6297 (2002).
26. Wang, J. et al. B7-H3 associated with tumor progression and epigenetic regulatory activity in cutaneous melanoma. *J. Invest. Dermatol.* **133**, 2050–2058 (2013).
27. Crispen, P. L. et al. Tumor cell and tumor vasculature expression of B7-H3 predict survival in clear cell renal cell carcinoma. *Clin. Cancer Res.* **14**, 5150–5157 (2008).
28. Zang, X. et al. Tumor associated endothelial expression of B7-H3 predicts survival in ovarian carcinomas. *Mod. Pathol.* **23**, 1104–1112 (2010).
29. Lee, Y. H. et al. Inhibition of the B7-H3 immune checkpoint limits tumor growth by enhancing cytotoxic lymphocyte function. *Cell Res.* **27**, 1034–1045 (2017).
30. Mahnke, K. et al. Induction of immunosuppressive functions of dendritic cells in vivo by CD4+CD25+ regulatory T cells: role of B7-H3 expression and antigen presentation. *Eur. J. Immunol.* **37**, 2117–2126 (2007).
31. Suh, W. K. et al. The B7 family member B7-H3 preferentially down-regulates T helper type 1-mediated immune responses. *Nat. Immunol.* **4**, 899–906 (2003).
32. Picarda, E., Ohaegbulam, K. C. & Zang, X. Molecular pathways: targeting B7-H3 (CD276) for human cancer immunotherapy. *Clin. Cancer Res.* **22**, 3425–3431 (2016).
33. Zhang, J. et al. B7-H3 is related to tumor progression in ovarian cancer. *Oncol. Rep.* **38**, 2426–2434 (2017).
34. Lin, H. et al. Host expression of PD-L1 determines efficacy of PD-L1 pathway blockade-mediated tumor regression. *J. Clin. Invest.* **128**, 805–815 (2018).
35. Abiko, K. et al. PD-L1 on tumor cells is induced in ascites and promotes peritoneal dissemination of ovarian cancer through CTL dysfunction. *Clin. Cancer Res.* **19**, 1363–1374 (2013).
36. Ling, V. et al. Duplication of primate and rodent B7-H3 immunoglobulin V- and C-like domains: divergent history of functional redundancy and exon loss. *Genomics* **82**, 365–377 (2003).
37. Prasad, D. V. et al. Murine B7-H3 is a negative regulator of T cells. *J. Immunol.* **173**, 2500–2506 (2004).
38. Kansy, B. A. et al. PD-1 status in CD8(+) T cells associates with survival and anti-PD-1 therapeutic outcomes in head and neck cancer. *Cancer Res.* **77**, 6353–6364 (2017).
39. Seaman, S. et al. Eradication of tumors through simultaneous ablation of CD276/B7-H3-positive tumor cells and tumor vasculature. *Cancer Cell.* **31**, 501–515 e8 (2017).
40. Alsaab, H. O. et al. PD-1 and PD-L1 checkpoint signaling inhibition for cancer immunotherapy: mechanism, combinations, and clinical outcome. *Front. Pharmacol.* **8**, 561 (2017).
41. Li, J. et al. Co-inhibitory molecule B7 superfamily member 1 expressed by tumor-infiltrating myeloid cells induces dysfunction of anti-tumor CD8(+) T cells. *Immunity* **48**, 773–86 e5 (2018).
42. Sun, Y. et al. B7-H3 and B7-H4 expression in non-small-cell lung cancer. *Lung Cancer* **53**, 143–151 (2006).
43. Dong, P., Xiong, Y., Yue, J., Hanley, S. J. B. & Watari, H. B7H3 as a promoter of metastasis and promising therapeutic target. *Front. Oncol.* **8**, 264 (2018).
44. Li, G., Quan, Y., Che, F. & Wang, L. B7-H3 in tumors: friend or foe for tumor immunity? *Cancer Chemother. Pharmacol.* **81**, 245–253 (2018).
45. Shalem, O. et al. Genome-scale CRISPR-Cas9 knockout screening in human cells. Science. **343**, 84–87 (2014).